Journal of Pathology Informatics 14 (2023) 100334

Contents lists available at ScienceDirect

Journal of Pathology Informatics

journal homepage: www.elsevier.com/locate/jpi

Cell projection plots: A novel visualization of bone marrow aspirate cytology

Taher Dehkharghanian [a,b], Youqing Mu [a], Catherine Ross [a,d], Monalisa Sur [a,d], H.R. Tizhoosh [c], Clinton J.V. Campbell [a,e,*]

[a] McMaster University, Hamilton, Canada
[b] University Health Network, Toronto, Canada
[c] Rhazes Lab, Artificial Intelligence & Informatics, Mayo Clinic, Rochester, MN, USA
[d] Juravinski Hospital and Cancer Centre, Hamilton, Canada
[e] William Osler Health System, Brampton, Canada

ARTICLE INFO

Keywords:
Digital pathology
Hematopathology
Machine learning
Artificial intelligence
Interpretable AI

ABSTRACT

Deep models for cell detection have demonstrated utility in bone marrow cytology, showing impressive results in terms of accuracy and computational efficiency. However, these models have yet to be implemented in the clinical diagnostic workflow. Additionally, the metrics used to evaluate cell detection models are not necessarily aligned with clinical goals and targets. In order to address these issues, we introduce novel, automatically generated visual summaries of bone marrow aspirate specimens called *cell projection plots* (CPPs). Encompassing relevant biological patterns such as neutrophil maturation, CPPs provide a compact summary of bone marrow aspirate cytology. To gauge clinical relevance, CPPs were inspected by 3 hematopathologists, who decided whether corresponding diagnostic synopses matched with generated CPPs. Pathologists were able to match CPPs to the correct synopsis with a matching degree of 85%. Our finding suggests CPPs can represent clinically relevant information from bone marrow aspirate specimens and may be used to efficiently summarize bone marrow cytology to pathologists. CPPs could be a step toward human-centered implementation of artificial intelligence (AI) in hematopathology, and a basis for a diagnostic-support tool for digital pathology workflows.

Introduction

Artificial intelligence (AI), particularly deep networks, has shown promise in digital pathology.[1,2] AI models assist with information extraction from digital whole slide images (WSIs) of pathology specimens, supporting and automating various aspects of pathology diagnostic workflows.[3] However, AI models have not yet been widely implemented in diagnostic hematopathology workflows.[4] In cytopathology, a number of AI models have been trained on bone marrow aspirate (BMA) images for cell detection and classification, including one from our group.[5–10] These models often return a nucleated differential count (NDC) as their output, where many types of individual bone marrow cells are classified and counted based on subtle morphological features.[11] While important for a number of clinical decision points in hematology, the NDC has limited value in some hematological diagnoses such as myelodysplastic syndrome (MDS), as it ignores the morphological complexities of BMA.[12] Additionally, such models do not relieve pathologists of the laborious task of viewing a large WSI to analyze thousands of cells. Therefore, in many cases, cell counts alone do not provide a summary of the complex information present in WSI needed to make a primary hematology diagnosis from BMA.

In digital pathology, AI models are often evaluated by measures such as accuracy, F1-score, and mean average precision (mAP)[13]; these are neither easy to interpret nor necessarily aligned with clinical problems and expectations in the medical field. Clinically meaningful evaluation of AI remains one of the challenges of its implementation in pathology.[14] Therefore, impressive performance in terms of computer science metrics does necessarily translate into a model's clinical utility. In pathology practice, the ultimate goal of cytopathology examination is not to find the most accurate bounding boxes in cell detection, but rather to glean biologically relevant information from a specimen to make a diagnosis that predicts biology, or patient outcomes. The necessity of clinical evaluation of medical AI has been well-emphasized.[15]

In the context of these limitations in practical utility and clinically relevant evaluations, we present a novel method to visualize cytological deep features extracted from BMA images to hematopathologists. We combined deep feature extraction and dimensionality reduction to create a compact visual summary of BMA slides, called a *cell projection plot* (CPP). Deep features are real-valued vectors generated by deep networks, which have been extensively used for image representation in both cytology and histopathology.[16–20] Dimensionality reduction has an established usage in

* Corresponding author at: William Osler Health System, S.3.421 – 2100, Bovaird Dr E, Brampton, ON L6R 3J7, Canada.
E-mail address: campbecj@mcmaster.ca (C.J.V. Campbell).

http://dx.doi.org/10.1016/j.jpi.2023.100334
Received 21 March 2023; Received in revised form 25 July 2023; Accepted 26 August 2023
Available online 30 August 2023

visual analytics.[21] Therefore, a combination of deep feature extraction and dimensionality reduction is an intuitive approach to represent BMAs to pathologists in a user-friendly and interpretable way. Although dimensionality reduction has been used in the field of hematopathology for deep feature evaluation,[22,23] its potential for developing clinical tools has yet to be explored.

In our previous work, we have described a system for detection and classification of BMA cells.[6] In this work, we develop CPPs by: (a) re-purposing our published cell detection and classification model to serve as a feature extractor; (b) applying dimensionality reduction to visualize detected cells on a 2D plane; (c) evaluating the descriptive quality of CPPs by pathologists. Fig. 1 shows an overview of the approach implemented in this study. Our results suggest CPP can serve as an automatically generated visual summary of BMA cytology, capturing biologically and diagnostically relevant information. Therefore, CPPs provide additional insight into bone marrow cytology beyond NDC, and may eventually contribute to the development of AI-based compact representations for primary diagnosis in digital hematopathology workflows.

Materials and methods

The *College of American Pathologists* (CAP) has published guidelines for validating digital imaging workflows for diagnostic purposes.[24] In this study, we adopted these guidelines for evaluating CPP as a means for workflow augmentation in hematopathology. Accordingly, we had 3 hematopathologists evaluate CPP samples of 20 patients each; 60 BMA samples in total.

Data acquisition, slides, and patients

Sixty *May–Grünwald–Giemsa*-stained bone marrow aspiration WSIs were used in this study. These WSIs were scanned at 40× and stored in TIFF file format under Hamilton Research Ethics Board (HIREB) study protocol 7766-C. A custom software was developed to allow pathologists to view and evaluate WSIs and CPPs.

Cell detection and feature extraction

A pre-trained YOLO object detection model for bone marrow cell detection was used in this study.[6] YOLO detects and classifies bone marrow cells from bone marrow aspiration digital WSI. This model is composed of 3 parts: backbone, neck, and head. Feature extraction takes place in the backbone with its first output being used to produce deep feature vectors to represent each detected cell. Since detected cells are of different sizes, average pooling was applied to the corresponding regions to create a linear vector of size 256. This process is schematically depicted in Fig. 2.

Dimensionality reduction

The *Uniform Manifold Approximation and Projection* (UMAP) is a dimensionality reduction technique that preserves more of the global structure of the data compared to another popular dimensionality reduction algorithm, namely t-SNE.[25] UMAP was used to embed cell-specific deep feature vectors into 2 dimensions for visualization.

Cell projection plots

Although the pre-trained YOLO detection model detects 19 classes, only the following cells were included in this study: “blasts”, “promyelocytes”, “myelocytes”, “metamyelocytes”, “neutrophils”, “erythroblasts”, “lymphocytes”, “monocytes”, “plasma cells”, “eosinophils”, “basophils”, and “megakaryocytes”. Tissue tiles were sampled from digital bone marrow slides; the YOLO model was applied to tissue tiles to detect and classify cells, using the same pipeline described in our previous work.[6] 500 cells were sampled out of the detected cells in proportion to each cell type’s prevalence. “Megakaryocytes” were gathered by a modified method. Since megakaryocytes are not as abundant as other cell types and are often found in *thick regions* not useful for the NDC, more tissue tiles are needed to find megakaryocytes. Therefore, all tissue tiles in a WSI were used to detect an adequate number of megakaryocytes. The same YOLO model was used for this purpose.

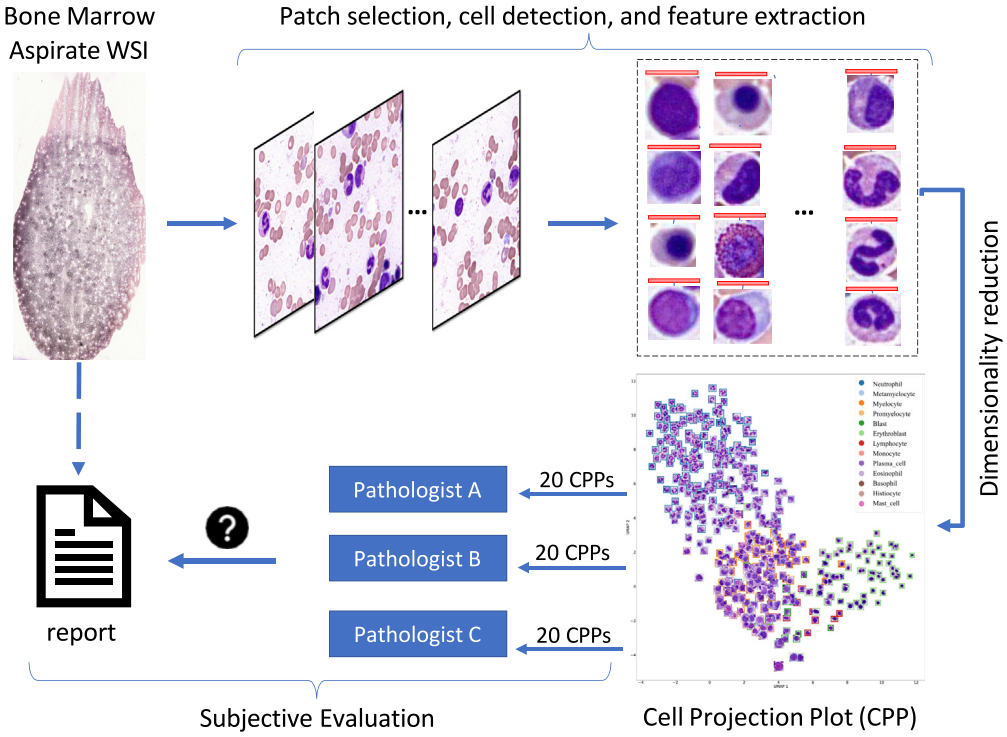

Fig. 1. Overview of CPP construction. First, bone marrow aspirate WSI tiles were analyzed by a deep network (i.e., YOLO) for cell detection and feature extraction. Then, deep feature vectors were embedded in a 2-dimensional space, and cells were visualized at their corresponding coordinates, to create CPPs. Three pathologists evaluated 60 CPPs (20 each), in order to assess whether CPPs provide diagnostically relevant information.

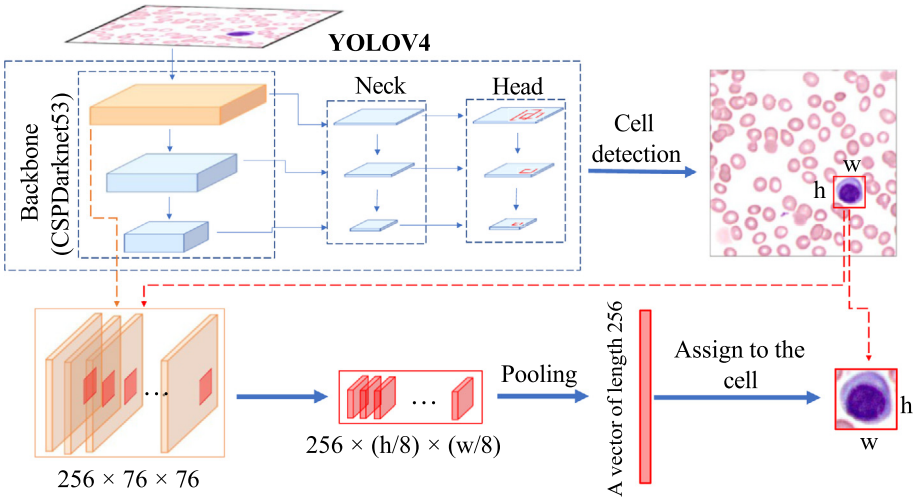

Fig. 2. Overview of the feature extraction process. Tissue tiles were analyzed by a YOLO model to detect cells and extract deep features. A deep feature vector was produced for each detected cell from the corresponding region on the feature map, i.e., the first output of the model's backbone. Average pooling was applied on the corresponding region to construct a deep feature vector of size 256 for each detected cell. These deep feature vectors represent cells.

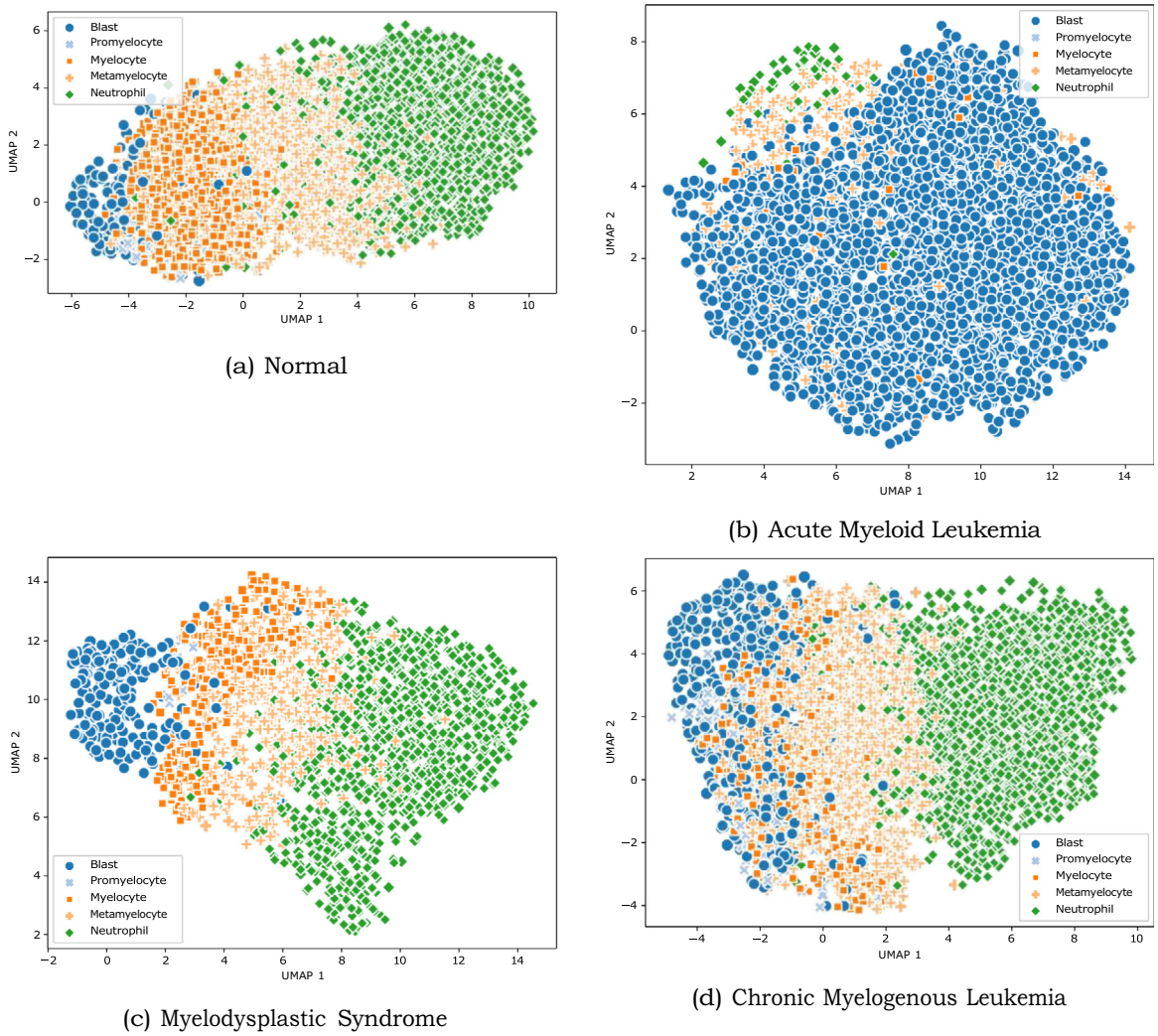

Fig. 3. Four UMAP plots showing the maturation of neutrophils: (a) orderly neutrophil maturation in a normal bone marrow aspirate WSI. The distribution of neutrophils and their precursors is in accordance with the expected biological maturation pattern, which suggests that the embeddings can be used to present semantically and clinically relevant patterns; (b) from an acute myeloid leukemia aspirate WSI where the blasts dominate the plot; (c) from a myelodysplastic syndrome aspirate WSI; (d) from a chronic myelogenous leukemia aspirate WSI, where there are abundant intermediate myeloid precursors. Of note, UMAP x and y coordinate values are arbitrary.

Particles

We designed an algorithm to find *particles* from WSI thumbnail images. We started by converting each thumbnail to a single-channel grayscale picture, which facilitates proper thresholding. We used Gaussian blurring to decrease the noise in this grayscale picture. After that, we employed thresholding to convert all pixels to binary (black and white) emphasizing the objects of interest, i.e., particles, for the contour-detection approach. To process this binary image, we also used mathematical morphology operation *erosion* to eliminate artifacts. Finally, we used OpenCV's[26] *findContours* function to determine the estimated contours of the particle. With particle contours in the thumbnail, we extracted particles from high-power images by coordinate conversion. Particles were shown to the pathologists so that they would have an estimate of the specimen's cellularity.

Cell projection plot evaluation design

Experiments were designed to solely evaluate the usability of CPPs. In order to prevent confirmation bias, the process was slightly gamified. 60 CPPs were shown to 3 pathologists; each pathologist reviewed 20 CPPs. For each CPP, either the real synopsis reported or a randomly sampled report was shown to the pathologists. To check CPP's descriptive quality, pathologists were asked to decide whether a displayed synopsis report was in concordance with their visual inspection of the corresponding CPP. Software was developed where pathologists could view and zoom in and out of CPPs. Prior to the evaluation, participating pathologists were informed about the process of CPP production. However, they had not experimented with CPP before the start of the evaluation process.

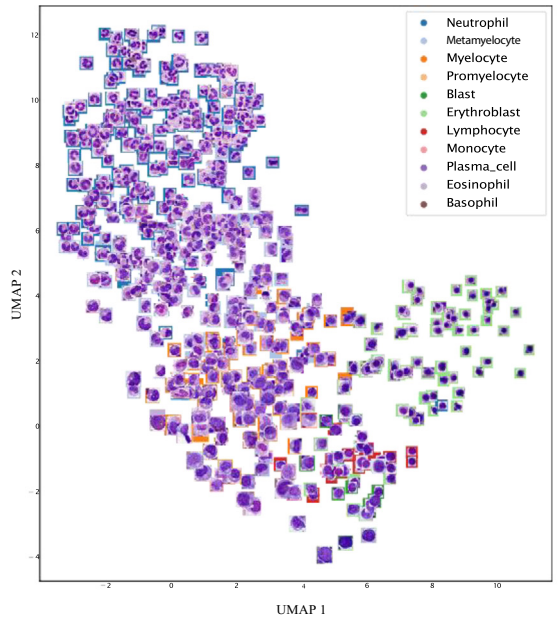

(a) Normal

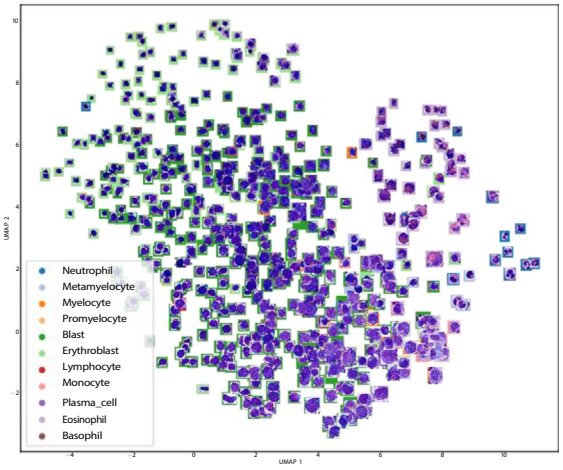

(b) Acute Myeloid Leukemia, Increased Eosinophils in bone marrow

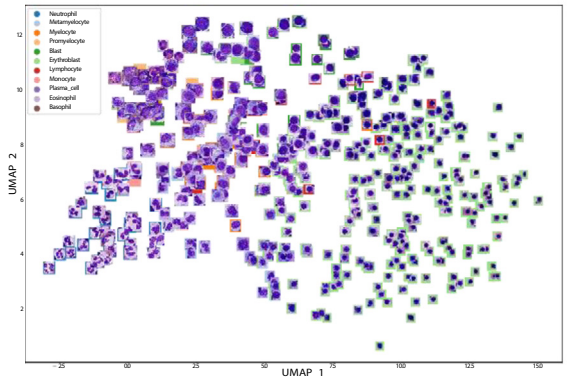

(c) Myelodysplastic Neoplasm

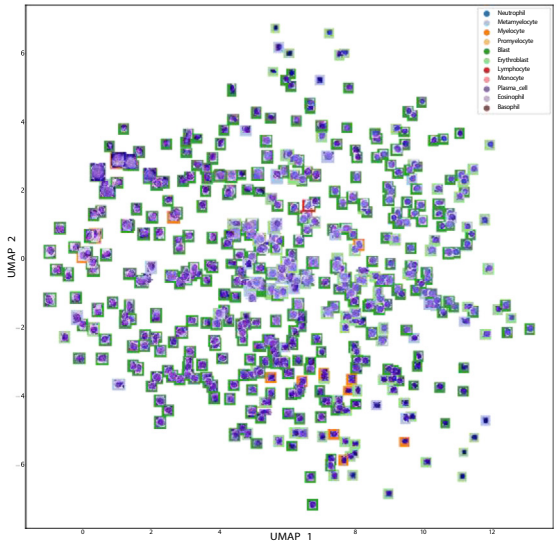

(d) Chronic Lymphocytic Leukemia

Fig. 4. Four sample Cell Projection Plots (CPP). CPPs were evaluated by pathologists: (a) from a normal BMA indicating an orderly distribution of cells; (b) an AML case with proportionally increased number of blasts and eosinophils; (c) from an MDS case (dysplastic erythropoiesis and granulopoiesis can be seen); (d) a CLL case where the object detection model misclassified lymphocytes as blasts.

Results

Cell projection plots

The goal of dimensionality reduction is to shrink the high-dimensional feature space so that it can be visualized while preserving the semantic relationship between individual embeddings, i.e., cells. To assess the quality of the YOLO embeddings (representing cells) used for CPPs, we assessed a well-described biological process in hematopoiesis: granulocytic (neutrophil) maturation. To this end, we used UMAP in cases of BMA WSI labeled as normal, acute myeloid leukemia (AML), myelodysplastic syndrome (MDS), and chronic myeloid leukemia. These example cases represent different expected biological states in terms of granulocytic maturation. A typical example of normal maturation is shown in Fig. 3a. This plot indicates a clear, continuous, and orderly granulocytic maturation pattern, with discernible neutrophil precursors subsets in expected biological proportion (blasts, promyelocytes, myelocytes, metamyelocytes, and neutrophils).

The plot in Fig. 3b is from a WSI labeled as AML, where one could see that blasts dominate the plot, indicating maturation arrest. Fig. 3c and d are generated from WSIs labeled as MDS and CML, respectively. In these cases, there is continuous granulocytic maturation, with varying proportions of blasts (MDS) and intermediate myeloid precursors (CML) as expected in these disease states. These observations suggested that generation and inspection of such visualizations—based on YOLO embeddings—could be useful for assessing semantically relevant patterns in BMA cytology.

More importantly, these experiments indicated that visualizing deep cell embeddings by dimensionality reduction is biologically and clinically relevant.

Next, we extended this concept to the entire cell population in a BMA, excluding megakaryocytes. CPPs are generated by adding individual cell images to the dimensionality reduction plots, thereby forming a compact representation of a BMA for visual assessment. Fig. 4a shows a typical CPP of a normal BMA, as well as a variety of typical hematopoietic diseases. In the normal CPP, for example, it can be seen that granulopoiesis and erythropoiesis are present, with granulopoiesis showing continuous maturation. Granulopoiesis is a distinct population moving from the bottom left to the top left with maturation, while erythropoiesis is a distinct population to the middle right of the CPP.

Fig. 4b shows a CPP of acute myeloid leukemia and increased eosinophils in BMA. The proportional increase in the number of blasts and eosinophils is evident. A CPP from MDS shows an expansion of erythropoiesis and dysplastic myelopoiesis, as would be expected (Fig. 4c), and a CPP for a chronic lymphocytic leukemia patient shows an expansion of abnormal lymphocytes (Fig. 4d). Although the model misclassified large lymphocytes as blasts in this case, this could be recognized and intercepted by hematopathologists. Therefore, these findings suggested that pathologists can quickly review these CPPs as a compact representation of BMA cytology, and also, as an interpretable implementation of AI in BMA cytology.

Megakaryocytes were shown to hematopathologists in a CPP that did not include other cell types, due to their larger size and unique biological significance. Fig. 5a shows a megakaryocyte CPP from a normal BMA, and Fig. 5b is from an MDS patient, where hyposegmented megakaryocytes can be seen.

Subjective evaluation

Next, we sought to assess whether pathologists may use a CPP as a tool in BMA cytology. Hematopathologists were asked to decide whether a shown synopsis belongs to the corresponding CPP. Among all 60 slides, the real synopsis report was shown in 26 cases (43.33%). In 46 out of 60 cases (76.67%), pathologists correctly decided whether the CPP matches the shown synopsis or not, as shown in the confusion matrix shown in Fig. 6. It is important to note that pathological evaluation is a subjective task, particularly BMA cytology, that expectedly suffers from inter- and intraobserver variability. Additionally, randomly selected synopses were considered to be negative cases. Therefore, some of those randomly selected synopses might have been semantically similar to the real synopsis. Upon examination of the 5 false-positive cases (random but deemed match), it was found that in all those cases, the shown synopsis was similar to the real synopsis. Consequently, the accuracy could be adjusted to 85% with no false-positive cases.

Discussion

In this work, we presented CPPs, a new visualization scheme to efficiently and compactly represent the information gathered by an objection detection model from BMA WSI. The usability of CPPs was

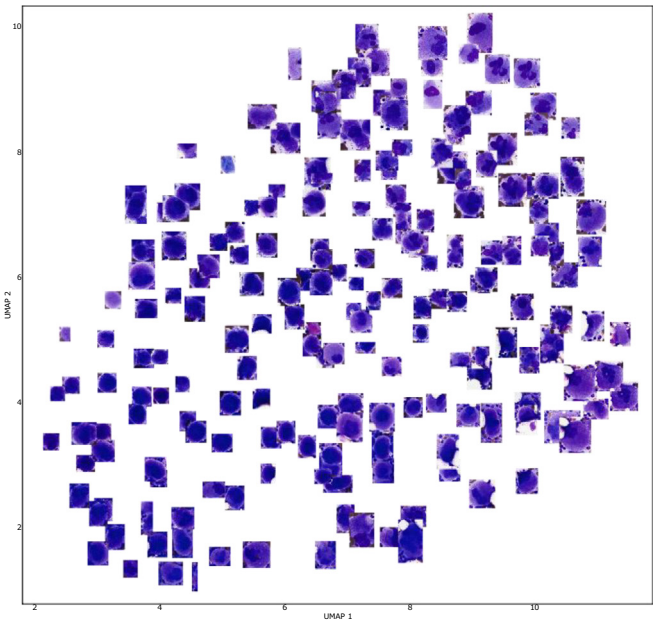

(a) Normal

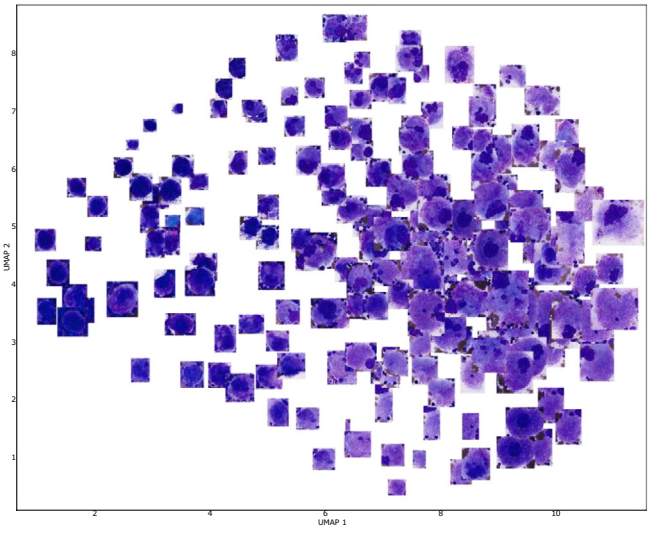

(b) Myelodysplastic Syndrome

Fig. 5. Two sample CPPs for megakaryocytes. CPPs were evaluated by pathologists: (a) from a normal BMA; (b) a bone marrow aspirate labeled as MDS with atypically lobulated megakaryocytes, including hyper- and hypolobulated forms.

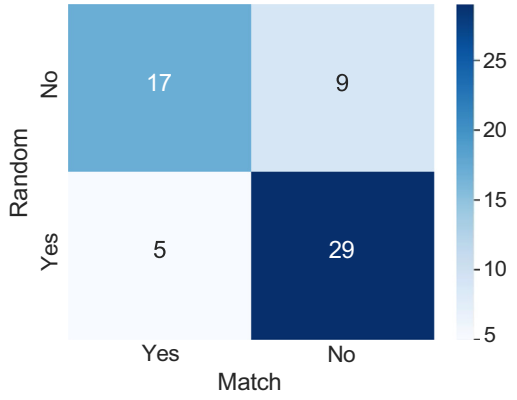

Fig. 6. The confusion matrix for the synopsis matching experience. Pathologists were asked to decide whether a displayed synopsis is for the shown CPP or not.

evaluated by hematopathologists through synopsis-matching experiments. This evaluation took place in a medically relevant setting. However, we did not provide any additional patient information to the pathologist other than the CPP itself (as a summary of the WSI). This limited amount of information makes diagnosis particularly difficult. In real-world clinical practice, pathology, especially hematopathology, is *multimodel*, where significant ancillary data, such as clinical history, flow cytometry, and molecular data are required to make a final diagnosis.[27] However, our evaluating pathologists did not have access to data beyond morphology in this type of controlled evaluation. Additionally, the task of BMA reporting is subjective in nature. Thus, 2 pathologists could have different interpretations of the same BMA slide. Therefore, even if both the digitization process and the AI model were perfect, it would not be expected that the evaluating pathologist to completely agree on a slide synopsis, which was deemed as ground truth in this study. However, at the same time, pathologists would not be expected to differ significantly. Additionally, in our study, there were 5 randomly selected synopses that were falsely deemed matching to the CPP. However, upon examining these shown synopses with the actual ones, we found that the shown and actual synopses were quite similar, with a similar primary diagnosis. Therefore, it can be said that they are true-positive cases rather than false-positive cases, which could increase the synopsis matching accuracy to 85%.

AI's lack of explainability and interpretability is an obstacle to its acceptance for clinical use.[28–30] It is argued that the current post-hoc explainability approaches might be useful at patient-level decision-making.[31] Therefore, explainability could be addressed while designing the AI workflow implementation. Using CPPs, pathologists were able to assess the quality and clinical relevance of information presented by an AI model. Consequently, AI's lack of explainability could be circumvented by letting pathologists make the final decision using the information gathered by AI. Therefore, such implementation of AI is more explainable as opposed to an AI model making a diagnostic prediction per se. Furthermore, through the evaluation of cells labeled by the object detection model, pathologists could intercept and prevent misclassified cells from interfering with the diagnostic decision. For example, the object detection model used in this study in some cases classified abnormal lymphocytes as blasts,[6] however, this could be intercepted by pathologists using CPP. Additionally, one of the common concerns among pathologists is the possibility of their jobs being replaced by AI.[32] CPPs are pathologist-centric requiring physicians involved in the model's decision-making process, potentially acting as a clinical decision-support tool.

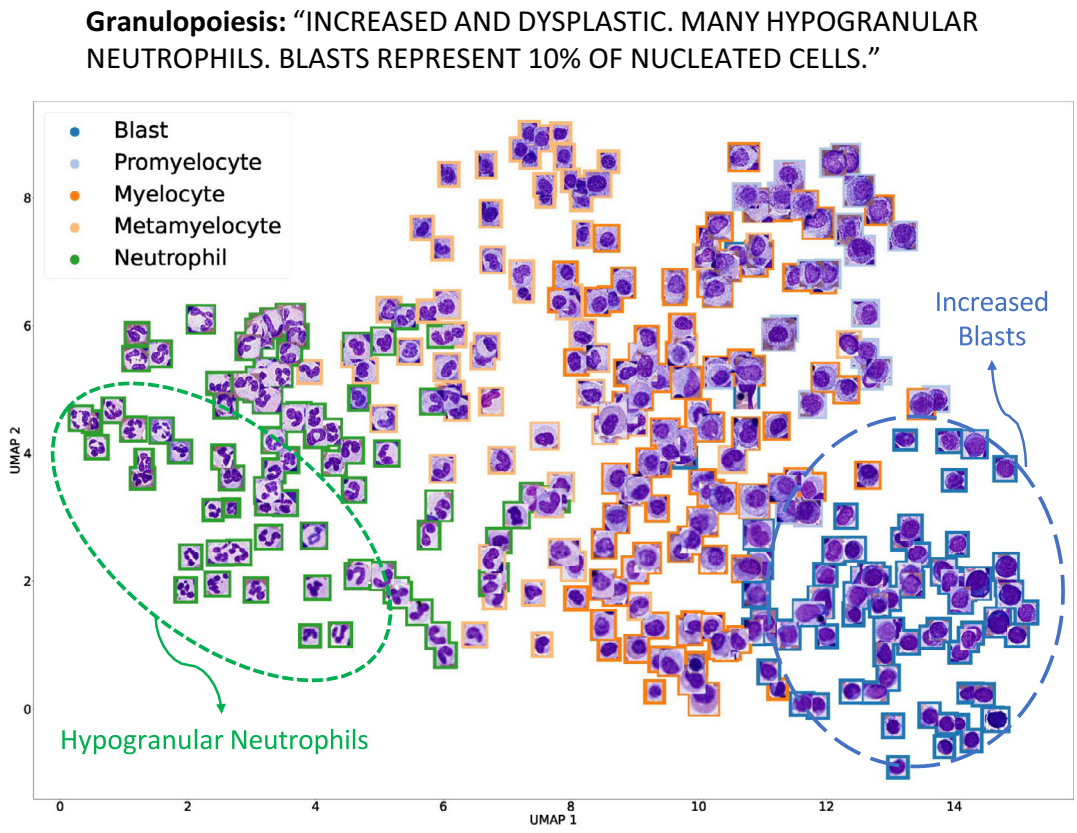

Fig. 7. Pathologist could annotate their findings on CPPs which are more transferable than multigigabyte-sized WSIs.

In summary, the CPP approach could be a useful tool to provide pathologists with the information obtained from object detection models in cytology. Additionally, CPPs coupled with reliable object detection models provide automatically generated supplementary information that could potentially augment the current diagnostic workflow. CPPs can be considered a preliminary step towards human-centered AI in cytopathology. CPP may also be used to make cytology reports more understandable for clinical stakeholders other than pathologists. As CPPs are more transferable than WSIs, pathologists could annotate their findings on CPPs and share them with other medical professionals, as shown in Fig. 7. Further investigation is required to measure the impact of CPPs if being used as a tool alongside WSIs to augment the digital cytology workflow. In this preliminary study, we aimed to explore CPP's potential to serve as a visual summary of bone marrow cytology, which was done through the synopsis matching experience. We acknowledge that this experiment has significant limitations. For instance, CPPs' performance in detection of different hematologic disorders such as MDS, AML, and MPN has not been investigated. For reference, we include a table of diagnostic labels/keywords for each synopsis assigned by one of the participating hematopathologists (supplemental tables 1–4),providing a broad overview of the diagnostic classification for each synopsis/CPP. Additionally, the synopsis matching accuracy provides limited information about CPPs' performance. We plan to address this shortcoming on a larger sample of WSIs in future studies.

Code availability

Code from this study is available at https://github.com/C-Campbell-Lab.

Funding

Funding for this work was provided by a Canadian Cancer Society BC Sparks Grant.

Author contributions

TD designed and conducted experiments analyzed data, and wrote the paper; HRT designed experiments, analyzed data, provided conceptual input, and contributed to writing the paper; YM provided conducted experiments, designed the software, and contributed to writing the paper; CJVC designed experiments, analyzed data, provided conceptual input and contributed to writing the paper. CJVC, CR, and MS reviewed and evaluated CPPs.

Data availability

The WSIs that support the findings of this study are not publicly available due to them containing information that could compromise research participant privacy/consent.

Declaration of Competing Interest

The authors declare the following financial interests/personal relationships which may be considered as potential competing interests:

Clinton J.V. Campbell, Hamid R. Tizhoosh, Taher Dehkharghanian, and Youqing Mu declare no competing interests.

Appendix A. Supplementary data

Supplementary data to this article can be found online at https://doi.org/10.1016/j.jpi.2023.100334.

References

1. Serag A, Ion-Margineanu A, Qureshi H, et al. Translational AI and deep learning in diagnostic pathology. Front Med 2019:6. https://doi.org/10.3389/fmed.2019.00185.
2. Tizhoosh HR, Pantanowitz L. Artificial intelligence and digital pathology: challenges and opportunities. J Pathol Inform 2018;9(1):38.
3. Beam AL, Kohane IS. Big data and machine learning in health care. JAMA 2018;319(13):1317. https://doi.org/10.1001/jama.2017.18391.
4. Chua IS, Gaziel-Yablowitz M, Korach ZT, et al. Artificial intelligence in oncology: path to implementation. Cancer Med 2021;10(12):4138–4149. https://doi.org/10.1002/cam4.3935.
5. Chandradevan R, Aljudi AA, Drumheller BR, et al. Machine-based detection and classification for bone marrow aspirate differential counts: initial development focusing on non-neoplastic cells. Lab Investig J Tech Methods Pathol 2020;100(1):98. https://doi.org/10.1038/S41374-019-0325-7.
6. Tayebi RM, Mu Y, Dehkharghanian T, et al. Automated bone marrow cytology using deep learning to generate a histogram of cell types. Commun Med 2022;2(1):45. https://doi.org/10.1038/s43856-022-00107-6.
7. Wu YY, Huang TC, Ye RH, et al. A hematologist-level deep learning algorithm (BMSNet) for assessing the morphologies of single nuclear balls in bone marrow smears: algorithm development. JMIR Med Inf 2020;8(4). https://doi.org/10.2196/15963.
8. Wang CW, Huang SC, Lee YC, Shen YJ, Meng SI, Gaol JL. Deep learning for bone marrow cell detection and classification on whole-slide images. Med Image Anal 2022;75, 102270. https://doi.org/10.1016/j.media.2021.102270.
9. Choi JW, Ku Y, Yoo BW, et al. White blood cell differential count of maturation stages in bone marrow smear using dual-stage convolutional neural networks. PLoS One 2017;12(12), e0189259. https://doi.org/10.1371/journal.pone.0189259.
10. Lewis JE, Shebelut CW, Drumheller BR, et al. An automated pipeline for differential cell counts on whole-slide bone marrow aspirate smears. bioRxiv 2022. https://doi.org/10.1101/2022.05.26.493480.
11. Lee SH, Erber WN, Porwit A, Tomonaga M, Peterson LC. ICSH guidelines for the standardization of bone marrow specimens and reports. Int J Lab Hematol 2008;30(5):349–364. https://doi.org/10.1111/j.1751-553X.2008.01100.x.
12. Sasada K, Yamamoto N, Masuda H, et al. Inter-observer variance and the need for standardization in the morphological classification of myelodysplastic syndrome. Leuk Res 2018;69:54–59. https://doi.org/10.1016/j.leukres.2018.04.003.
13. Hicks SA, Strümke I, Thambawita V, et al. On evaluation metrics for medical applications of artificial intelligence. Sci Rep 2022;12(1):5979. https://doi.org/10.1038/s41598-022-09954-8.
14. Radakovich N, Nagy M, Nazha A. Artificial intelligence in hematology: current challenges and opportunities. Curr Hematol Malig Rep 2020;15(3):203–210. https://doi.org/10.1007/s11899-020-00575-4.
15. Park Y, Jackson GP, Foreman MA, Gruen D, Hu J, Das AK. Evaluating artificial intelligence in medicine: phases of clinical research. JAMIA Open 2020;3(3):326–331. https://doi.org/10.1093/jamiaopen/ooaa033.
16. Sirinukunwattana K, Aberdeen A, Theissen H, et al. Artificial intelligence–based morphological fingerprinting of megakaryocytes: a new tool for assessing disease in MPN patients. Blood Adv 2020;4(14):3284–3294. https://doi.org/10.1182/BLOODADVANCES.2020002230.
17. Basak H, Kundu R, Chakraborty S, Das N. Cervical cytology classification using PCA and GWO enhanced deep features selection. SN Comput Sci 2021;2(5):1-17. https://doi.org/10.1007/S42979-021-00741-2.
18. Sahlol AT, Kollmannsberger P, Ewees AA. Efficient classification of white blood cell leukemia with improved swarm optimization of deep features. Sci Rep 2020;10(1):2536. https://doi.org/10.1038/s41598-020-59215-9.
19. Riasatian A, Babaie M, Maleki D, et al. Fine-Tuning and training of densenet for histopathology image representation using TCGA diagnostic slides. Med Image Anal 2021;70, 102032. https://doi.org/10.1016/j.media.2021.102032.
20. Dehkharghanian T, Rahnamayan S, Riasatian A, et al. Selection, visualization, and interpretation of deep features in lung adenocarcinoma and squamous cell carcinoma. Am J Pathol 2021;191(12):2172–2183. https://doi.org/10.1016/J.AJPATH.2021.08.013/ATTACHMENT/7711F794-9E0A-472B-979C-279E9E3DB554/MMC3.DOCX.
21. Yuan J, Chen C, Yang W, Liu M, Xia J, Liu S. A survey of visual analytics techniques for machine learning. Computat Visual Media 2020;7(1):3-36. https://doi.org/10.1007/S41095-020-0191-7.
22. Matek C, Krappe S, Münzenmayer C, Haferlach T, Marr C. Highly accurate differentiation of bone marrow cell morphologies using deep neural networks on a large image data set. Blood 2021;138(20):1917–1927. https://doi.org/10.1182/blood.2020010568.
23. Sidhom JW, Siddarthan IJ, Lai BS, et al. Deep learning for diagnosis of acute promyelocytic leukemia via recognition of genomically imprinted morphologic features. npj Precision Oncology 2021;5(1):38. https://doi.org/10.1038/s41698-021-00179-y.
24. Evans AJ, Brown RW, Bui MM, et al. Validating whole slide imaging systems for diagnostic purposes in pathology: guideline update from the College of American Pathologists in collaboration with the American Society for Clinical Pathology and the Association for Pathology Informatics. Arch Pathol Lab Med 2021. https://doi.org/10.5858/arpa.2020-0723-CP.
25. McInnes L, Healy J, Melville J. *UMAP: Uniform Manifold Approximation and Projection for Dimension Reduction.* 2018.
26. Bradski G. The OpenCV library. Doctor Dobbs J 2000;25:120–126.
27. Dunphy CH. Applications of flow cytometry and immunohistochemistry to diagnostic hematopathology. Arch Pathol Lab Med 2004;128(9):1004–1022. https://doi.org/10.5858/2004-128-1004-AOFCAI.

28. Evans T, Retzlaff CO, Geißler C, et al. The explainability paradox: challenges for xAI in digital pathology. Futur Gener Comput Syst 2022;133:281–296. https://doi.org/10.1016/j.future.2022.03.009.
29. McKay F, Williams BJ, Prestwich G, Bansal D, Hallowell N, Treanor D. The ethical challenges of artificial intelligence-driven digital pathology. J Pathol Clin Res 2022;8(3):209–216. https://doi.org/10.1002/cjp2.263.
30. Kundu S. AI in medicine must be explainable. Nat Med 2021;27(8):1328. https://doi.org/10.1038/s41591-021-01461-z.
31. Ghassemi M, Oakden-Rayner L, Beam AL. The false hope of current approaches to explainable artificial intelligence in health care. The Lancet Digital Health 2021;3(11):e745–e750. https://doi.org/10.1016/S2589-7500(21)00208-9.
32. Chauhan C, Gullapalli RR. Ethics of AI in pathology. Am J Pathol 2021;191(10):1673–1683. https://doi.org/10.1016/j.ajpath.2021.06.011.